Full title: Evaluation of CRISPR gene-editing tools in zebrafish

Short title: CRISPR gene-editing tools in zebrafish

José M. Uribe-Salazar[1,2], Gulhan Kaya[1], Aadithya Sekar[1], KaeChandra Weyenberg[1], Cole Ingamells[1], Megan Y. Dennis[1,2†]

[1]Genome Center, MIND Institute, and Department of Biochemistry & Molecular Medicine, University of California, Davis, CA, USA; [2]Integrative Genetics and Genomics Graduate Group, University of California, Davis, CA, USA

[†]Corresponding author:

Megan Y. Dennis, Ph.D.

University of California, Davis, School of Medicine

One Shields Avenue

Genome Center, 4303 GBSF

Davis, CA 95616

Email: mydennis@ucdavis.edu

Keywords: *Danio rerio*, zebrafish, CRISPR, Cas9, gene knockout, CIRCLE-seq, RNA-seq.

1 **ABSTRACT**

2 Background: Zebrafish have practical features that make them a useful model for higher-

3 throughput tests of gene function using CRISPR/Cas9 editing to create 'knockout' models. In

4 particular, the use of G_0 mosaic mutants has potential to increase throughput of functional studies

5 significantly but may suffer from transient effects of introducing Cas9 via microinjection.

6 Further, a large number of computational and empirical tools exist to design CRISPR assays but

7 often produce varied predictions across methods leaving uncertainty in choosing an optimal

8 approach for zebrafish studies.

9 Methods: To systematically assess accuracy of tool predictions of on- and off-target gene editing,

10 we subjected zebrafish embryos to CRISPR/Cas9 with 50 different guide RNAs (gRNAs)

11 targeting 14 genes. We also investigate potential confounders of G_0-based CRISPR screens by

12 screening control embryos for spurious mutations and altered gene expression.

13 Results: We compared our experimental *in vivo* editing efficiencies in mosaic G_0 embryos with

14 those predicted by eight commonly used gRNA design tools and found large discrepancies

15 between methods. Assessing off-target mutations (predicted *in silico* and *in vitro*) found that the

16 majority of tested loci had low *in vivo* frequencies (<1%). To characterize if commonly used

17 'mock' CRISPR controls (larvae injected with Cas9 enzyme or mRNA with no gRNA) exhibited

18 spurious molecular features that might exacerbate studies of G_0 mosaic CRISPR knockout fish,

19 we generated an RNA-seq dataset of various control larvae at 5 days post fertilization. While we

20 found no evidence of spontaneous somatic mutations of injected larvae, we did identify several

21 hundred differentially-expressed genes with high variability between injection types. Network

22 analyses of shared differentially-expressed genes in the 'mock' injected larvae implicated a

23 number of key regulators of common metabolic pathways, and gene-ontology analysis revealed

24 connections with response to wounding and cytoskeleton organization, highlighting a potentially

1   lasting effect from the microinjection process that requires further investigation.

2   <u>Conclusion</u>: Overall, our results provide a valuable resource for the zebrafish community for the

3   design and execution of CRISPR/Cas9 experiments.

4

5   **BACKGROUND**

6   Zebrafish (*Danio rerio*) are increasingly used to rapidly and robustly characterize gene functions

7   [1–4]. Features that make this model attractive over other classic vertebrate systems include

8   external fertilization, rapid development, a large number of progeny, embryonic transparency,

9   small size, and the availability of effective gene-editing tools [3, 5–12]. Continuous

10   improvements of CRISPR editing in zebrafish have allowed efficient targeting of multiple genes

11   simultaneously leading to rapid generation of either mosaic (G_0) or stable mutant lines and

12   subsequent characterizations of phenotypes [8, 13–19]. Such mutants have subsequently been

13   used to test candidate genes associated with human diseases and developmental features [20].

14   The trend towards more affordable higher-throughput protocols using zebrafish requires a careful

15   evaluation of methods used for the design of CRISPR-based genetic screens and potential

16   confounders that may arise from the microinjection process that could artificially impact

17   phenotypes.

18

19   New and creative CRISPR-based approaches in zebrafish address biological questions related to

20   developmental processes (e.g., cell-lineage tracing) as well as gene functions (e.g., epigenome

21   editing and targeted mutagenesis, reviewed in [21]). In the latter application, important factors in

22   generating CRISPR gene knockouts include predicting/maximizing 'on target' Cas9 cleavage

23   activity, predicting/minimizing unintended 'off-target' editing events, and rapidly detecting

1   small insertions or deletions (indels). Presence of indels at candidate loci can be determined in an

2   affordable manner via a number of approaches (reviewed in [22]), ranging from simple

3   identification of heteroduplexes—arising from multiple alleles coexisting in the sampled DNA—

4   visualized using a polyacrylamide gel electrophoresis (PAGE) [23] to more sophisticated

5   sequencing approaches that precisely identify and quantify mutant alleles [14, 24]. On-target

6   activity of a particular guide RNA (gRNA) can be predicted using tools that provide efficiency

7   scores, often defined by information gathered across empirical assays [25]. One relevant example

8   is CRISPRScan, a predictive-scoring system built from experimental zebrafish gene-editing data

9   based on multiple factors such as nucleotide GC and AT content and nucleosome positioning [9,

10   26]. Bioinformatic tools also exist that define potential regions prone to off-target edits mainly

11   based on sequence similarity and the type/amount of mismatches relative to the on-target region

12   [26]. More recently, several methods have been devised to experimentally identify off-target

13   cleavage sites (reviewed in [27]), including CIRCLE-Seq [28] and GUIDE-seq [29], that do not

14   depend on prior sequence similarity information. These approaches are meant to provide a blind

15   assessment of editing sites but do not necessarily reflect the *in vivo* activity of on-target activity

16   of the CRISPR/Cas9 complex.

17

18   Previous studies have shown CRISPR off-target activity *in vivo* to be relatively low in zebrafish

19   [8, 12, 18]. A cross-generational study identified no inflation of transmitted *de novo* single-

20   nucleotide mutations due to CRISPR-editing using exome sequencing and a stringent

21   bioinformatic pipeline [30] in a similar approach used to identify off-target mutations in mouse

22   trios [31, 32]. Other studies have observed off-target mutation rates ranging from 0.07 to 3.17%

23   in zebrafish by sequencing the top three to four predicted off-target regions based on sequence

1   homology [11, 12, 18]. Although off-target mutations should not significantly impact studies of

2   stable mutants, since unwanted mutations can be outcrossed out of studied lines relatively easily

3   [14, 21], they may be problematic in rapid genetic screens using G_0 mosaics that quickly test

4   gene functions in a single generation.

5

6   The increasing number of tools available for the design and execution of CRISPR screens

7   provide an important resource to the zebrafish community. Here, we assayed different available

8   CRISPR on- and off-target prediction methods using empirical data from Cas9-edited zebrafish

9   embryos. We quantified CRISPR cleavage efficiencies *in vivo* employing a variety of

10   experimental approaches and used these results to compare the accuracy of *in silico* and *in vitro*

11   tools for predicting Cas9 on- and/or off-target activity. Finally, to examine potential confounders

12   that may arise from microinjection of Cas9 into embryos on resulting phenotypes, we assayed G_0

13   'mock' negative control embryos injected with a buffer containing either Cas9 enzyme or mRNA

14   in the absence of gRNAs by performing RNA-seq and obtained a list of genes with significant

15   differential expression versus uninjected wild-type siblings. In all, these results will serve as a

16   useful resource to the research community as larger-scale G_0 CRISPR screens become more

17   common in assaying gene functions in zebrafish.

18

19   **RESULTS**

20   **Identification of CRISPR-induced indels in zebrafish**

21   We generated a dataset of experimentally confirmed indels within 14 protein-coding genes from

22   injected NHGRI-1 wild-type zebrafish larvae targeted by 50 gRNAs (2–4 different gRNAs/target

23   gene, assembled through the annealing of crRNA:tracrRNA) (Figure 1A, Supplementary Tables

1   1 and 2). These 50 gRNAs were designed using CRISPRScan [26] and include a range of

2   predicted editing efficiencies (mean 57.6, range 23–83). To obtain experimental *in vivo* editing

3   efficiency values for each gRNA, DNA extracted from a pool of 20 G_0 mutant embryos —

4   generated via microinjections of individual gRNAs at the one-cell stage and harvested at five

5   days post-fertilization (dpf)— and ~200 bp regions surrounding predicted cut sites for all gRNAs

6   were amplified and Illumina sequenced. To extract the proportion of reads carrying indel alleles,

7   we used *CrispRVariants* [35] with uninjected batch siblings DNA as reference (Supplementary

8   Table 2 for all scores obtained). From this, we inferred an *in vivo* 'efficiency score', calculated as

9   the percentage of DNA from injected embryos harboring indels compared to uninjected batch

10   siblings (Figure 1B).

11

12   To compare our efficiency scores with those produced from Sanger-based tools, we also

13   amplified and sequenced ~500 bp fragments surrounding the targeted sites from the same DNA.

14   We extracted the percentage of indels using two different tools that deconvolve major mutations

15   and their frequencies within Sanger traces—Tracking of Indels by DEcomposition (TIDE) [33]

16   and Inference from CRISPR Edits (ICE) [34] (Figure 1B). Briefly, these tools use the gRNA

17   sequence to predict the cutting site in the control trace, map the sample trace to this reference,

18   identify indels by deconvolving all base reads at each position, and provide a frequency of the

19   indel spectrum [33, 34]. As previously reported [34], both tools provided positively correlated *in*

20   *vivo* scores across all gRNAs (Spearman ρ= 0.87, *p*= 6.78x10^{-15}) with an average score

21   difference of 8.8±12.1 between tools (Figure 1C). We noted a higher correlation between tools in

22   scores below the median (Spearman ρ= 0.96, *p*= 1.23x10^{-13}) than above the median (Spearman

23   ρ= 0.65, *p*= 0.00072; Figure 1C), suggesting that the deconvolution process in both tools is more

1 accurate when fewer molecules from the pool carry indels. Both ICE and TIDE efficiency scores

2 were correlated with our Illumina-based editing scores (ICE: Spearman ρ= 0.88, p= 9.14x10^{-16};

3 TIDE: Spearman ρ= 0.59, p= 7.33x10^{-6}; Figure 1D), though they significantly underestimated

4 editing efficiencies with, for example, Illumina estimates 19.4±16.3 higher than ICE estimated

5 scores (Figure 1D). Based on its higher correlation, we reported Sanger-based ICE *in vivo* scores

6 for the rest of this study.

7

8 To ascertain consistency of editing efficiencies across embryos, we also repeated microinjections

9 for four gRNAs targeting a single gene (*srgap2*) and assessed *in vivo* efficiencies scores of 20

10 individual larvae using the ICE tool. This resulted in low variance across injections and relative

11 parity of efficiencies versus results from our pooled-larvae DNA preparations (e.g., low

12 efficiency gRNA targeting exon 2; average±SE ICE score in individual larvae 18.9±3.3 versus

13 an ICE score of 13 in pooled larvae and a high efficiency gRNA targeting exon 4; average±SE in

14 individual larvae 69.2±5.3 ICE score versus an ICE score of 68 in pooled larvae).

15

16 A quicker and more affordable approach to quantify CRISPR cleavage efficiency is via PAGE,

17 which takes advantage of the heteroduplexes produced from DNA harboring a mosaic mix of

18 different types of indel mutations [23]. We performed PAGE on ~200 bp regions surrounding the

19 predicted target site for each gRNA and quantified the PCR 'smear' intensity ratio of injected

20 versus uninjected controls (see Methods). These intensity ratios were weakly correlated with our

21 Illumina- (Spearman ρ= 0.37, p= 0.016) and ICE-estimated scores (Spearman ρ= 0.38, p= 0.018,

22 Figure 1E), indicating that accurate quantitative efficiencies cannot be directly deduced from

23 PAGE but that the intensity of PCR 'smear' does qualitatively convey CRISPR-cleavage

1 efficiency.
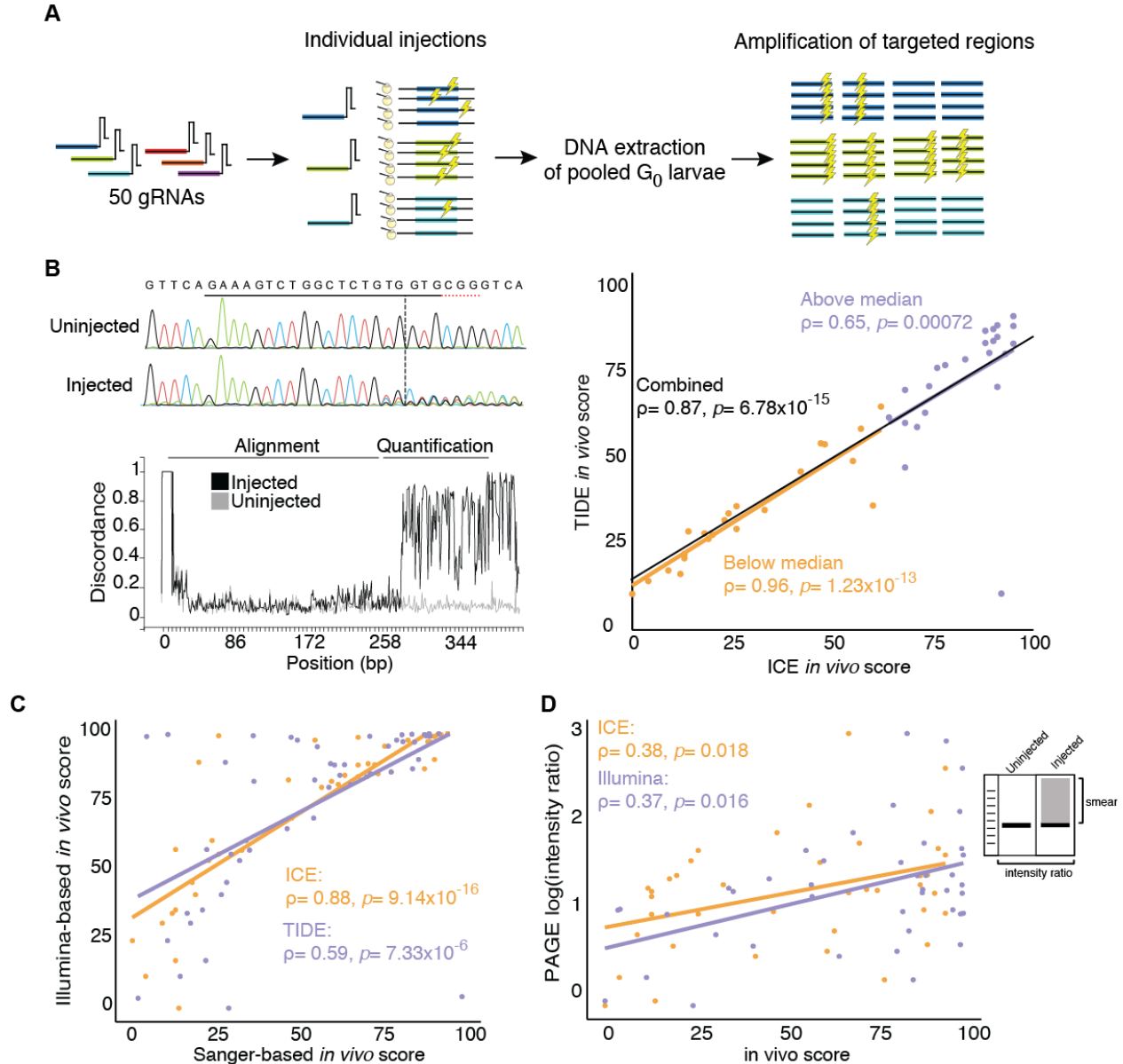
Figure 1. Workflow for the evaluation of CRISPR cleavages in NHGRI-1 zebrafish embryos. (A) The cartoon depicts our experiment, which included 50 gRNAs individually microinjected into one-cell stage embryos, DNA extracted from 20 pooled G_0 larvae, and genomic regions targeted by the gRNA amplified. Lightning symbols represent a cleavage event. (B) An *in vivo* score was obtained from the Sanger sequencing traces using the ICE and TIDE tools, with an example output from ICE pictured. (C) Scores for the two tools were plotted with values below the median in orange and above the median in purple. (D) Scores from ICE and TIDE tools were compared to mosaicism percentages from Illumina sequencing of the same regions. (E) From the PAGE, an empirical intensity ratio was obtained and compared to the *in vivo* scores from Illumina and Sanger sequencing (ICE). Spearman correlations results are shown in the scatter plots with the line of best fit included.

1 **Accuracy of CRISPR on-target predictions by *in silico* methods**

2 We next compared the accuracy of CRISPR on-target predictions computed by several published

3 algorithms, including our chosen design tool CRISPRScan [26] (among the most popular tools

4 used by the zebrafish community), CHOPCHOP [35–37] using two different scoring methods

5 [38] [39] (among the most widely-used tool generally), E-CRISP [40], CRISP-GE [41], CCTop

6 [42], CRISPRon [43], DeepSpCas9 [44], as well as the design tool from Integrated DNA

7 Technologies (IDT, www.idtdna.com). Additionally, to assess if strain variability may have

8 impacted our analysis—since all prediction tools used the Tübingen-derived reference genome

9 (GRCz11) [4] whereas our study was performed in the NHGRI-1 strain (a cross between wild-

10 type strains AB and Tübingen [46])—we obtained re-calculated CRISPRScan scores for our

11 gRNAs using a modified zebrafish reference that included known NHGRI-1 variants [46] (now

12 available as an additional reference in the tool browser at www.crisprscan.org). We then

13 compared all *in silico* predicted efficiency scores to our *in vivo* mutagenesis from Illumina

14 sequencing and ICE and observed a generalized underestimation of editing efficiency (Figure

15 2A). Strikingly, only scores predicted by CRISPRScan exhibited significant, albeit weak,

16 correlation with *in vivo* scores. Further, the correlation with Illumina-based scores was

17 significant only when using our NHGRIzed reference (Spearman $\rho= 0.31$, $p= 0.028$; Figure 2B),

18 though CRISPRScan scores were highly concordant with those obtained using the Tübingen-

19 derived reference (Spearman $\rho= 0.88$, $p= 5.02 \times 10^{-17}$; Figure 2B), with an average difference

20 between scores of 4.2 ± 4.6 (range 0–31) (Supplementary Table 2). CHOPCHOP values exhibited

21 correlations with scores from four other *in silico* tools (E-CRISP, CRISPRon, DeepSpCas9, IDT)

22 but none were concordant with our *in vivo* results (Figure 2B). Additionally, two tools that utilize

23 deep learning methods (CRISPRon and DeepSpCas9) were significantly correlated with each

1   other but failed to predict *in vivo* editing efficiencies in our assay (Figure 2B). Thus, despite the

2   research community broadly adapting all methods for designing gRNAs, there is little consensus

3   in predicting activity of a particular gRNA among these tools. Based on our results, we

4   recommend using CRISPRScan for choosing gRNAs in zebrafish experiments.

5
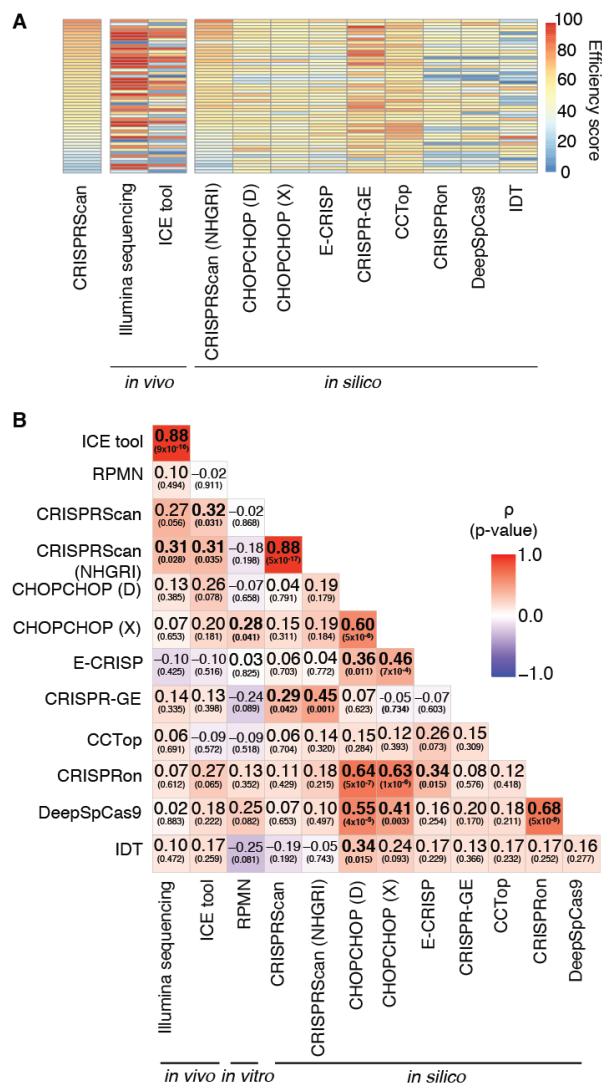
6

7   **Figure 2. Correlation of on-target efficiencies calculated using different methods. (A)** Heatmap of the efficiency
8   scores obtained from the design tool (CRISPRScan), *in silico* prediction tools, and cutting cleavages obtained *in vivo*
9   using Illumina sequencing and a deconvolution tool from Sanger sequencing [34] for 50 gRNAs. Each box
10   represents a gRNA and the efficiency scores range from 0 (blue) to 100 (red). **(B)** Spearman correlations between all
11   efficiency scores from *in silico* predictions, an *in vitro* protocol [28], and *in vivo* cutting assays. Each box includes
12   the correlation result with the *p-value* in parenthesis. The color of the boxes represent the correlation values, ranging
13   between -1 (blue) and 1 (red). CHOPCHOP scores were obtained using two different scoring methods, CHOPCHOP
14   (D) (based on [39]) and CHOPCHOP (X) (based on [40]).

1 **Accuracy of CRISPR on-target predictions by an *in vitro* method**

2 Next, we evaluated the possibility of using the *in vitro* protocol CIRCLE-seq [28], an approach

3 designed to identify target sites of a given gRNA by subjecting naked genomic DNA to Cas9

4 enzyme/gRNA cleavage followed by Illumina sequencing, to obtain an editing efficiency score.

5 It is important to emphasize that such *in vitro* assays are not designed for predicting on-target

6 editing efficiencies. Nevertheless, we sought to understand if such an approach *could* be used for

7 this purpose. We tested individually the 50 gRNAs described above using the CIRCLE-seq

8 protocol [46], following the standard recommendations, and computed a log enrichment score

9 normalized by the sequence library size, termed reads per million normalized (RPMN) (see

10 Methods). We found that *in vitro*-obtained enrichment scores were not correlated with *in vivo*

11 efficiencies (Illumina: Spearman ρ= 0.10, *p*= 0.494; ICE: Spearman ρ= -0.02, *p*= 0.911, Figure

12 2B) or with *in silico* predictions, with the exception of CHOPCHOP using the scoring method by

13 [39] (Figure 2). This indicates that the CIRCLE-seq assay does not necessarily predict on-target

14 CRISPR cleavage activity, at least quantitatively. Previous work from *in vivo* CRISPR studies of

15 zebrafish suggests that increased GC-content predicts increased activity of gRNAs [26].

16 Examining GC content of our tested gRNAs, ranging from 31.8 to 77.3%, we observed a positive

17 correlation with CRISPRScan *in silico* scores (linear model: beta= 68.18, *p*= 0.003, adjusted-r^2=

18 0.16) and CIRCLE-seq *in vitro* RPMN scores (linear model: beta= 6.4, *p*= 0.006, adjusted-r^2=

19 0.14) (Supplementary Figures 1A and B); however, our experimentally determined *in vivo* scores

20 were not correlated with GC content (Illumina linear model: beta=-18.57, *p*= 0.689, adjusted-r^2=

21 -0.02; ICE linear model: beta=12.36, p= 0.817, adjusted-r^2= -0.02; Supplementary Figure 1C),

22 suggesting that additional variables should also be considered (e.g., depletion of A nucleotide

23 bases, nucleosome positioning or DNA accessibility [26, 45]).

1   **CRISPR off-target mutation prediction methods**

2   To avoid spurious phenotypes, off-target mutations should be minimized when choosing gRNAs

3   in CRISPR experiments. To characterize off-target mutations for our set of 50 gRNAs, we

4   queried predictions from *in silico* (CRISPRScan) and *in vitro* (CIRCLE-seq) methods.

5   CRISPRScan provides a list of predicted off-target sites (between 55 and 1,350, median 206.5;

6   Supplementary Table 3) for each gRNA within the zebrafish NHGRIzed reference genome

7   (GRCz11/danRer11) based on a cutting frequency determination (CFD) score that primarily

8   takes into account sequence similarity, location, and type of sequence mismatches [26, 38]. The

9   CIRCLE-seq empirical approach also produced variable numbers of sites (between 18 and 874,

10   median 113.5; Supplementary Table 3) per gRNA (defined as 'CIRCLE-seq sites') relative to the

11   control library digested solely with Cas9 enzyme. The number of off-target sites predicted by

12   CRISPRScan exhibited a significant, albeit weak, correlation with the number of CIRCLE-seq

13   sites per gRNA (Spearman ρ=0.33, *p*= 0.022, Figure 3A). Focusing on putatively impactful off-

14   target predictions, an average of 20±13% CRISPRScan-predicted and 64±7% CIRCLE-seq sites

15   per gRNA intersected at least one gene (Supplementary Table 3). The sites predicted *in silico* or

16   *in vitro* intersecting genes predominantly did not overlap with an average of 1.6±1.8 (range 0–7)

17   genes per gRNA overlapping between the two approaches for the same gRNA.

18
19   To verify if predicted off-target sites were subjected to *in vivo* Cas9 cleavage, we performed

20   Sanger sequencing of sites within genes identified *in silico* (n= 17) and *in vitro* (n= 20) for eight

21   gRNAs, an average of six regions per gRNA (see Supplementary Table 1 for description of

22   sites). Using the ICE tool, we found mosaic mutations at frequencies between 0 and 11%, with

23   23 out of the 37 sites evidencing indel frequencies below 1% (Figure 3B), and no differences

24   observed between off-target sites predicted by CRISPRScan or CIRCLE-seq (Mann-Whitney U=

1   175.5, p= 0.873; Figure 3B). To validate the accuracy of ICE at these low indel frequencies, we

2   again performed Illumina sequencing of predicted off-target sites for six of the eight evaluated

3   gRNAs (see Supplementary Table 1 for description) and found significant concordance in results

4   (0.29–7.62% of mosaicism; Spearman ρ= 0.83, p= 0.039; Figure 3C). The average difference in

5   mosaicism between ICE and Illumina was low (1.6±2.0), with ICE tending to slightly

6   underestimate indel frequencies, highlighting its utility to quickly and economically assess

7   predicted off-targets regions.

8
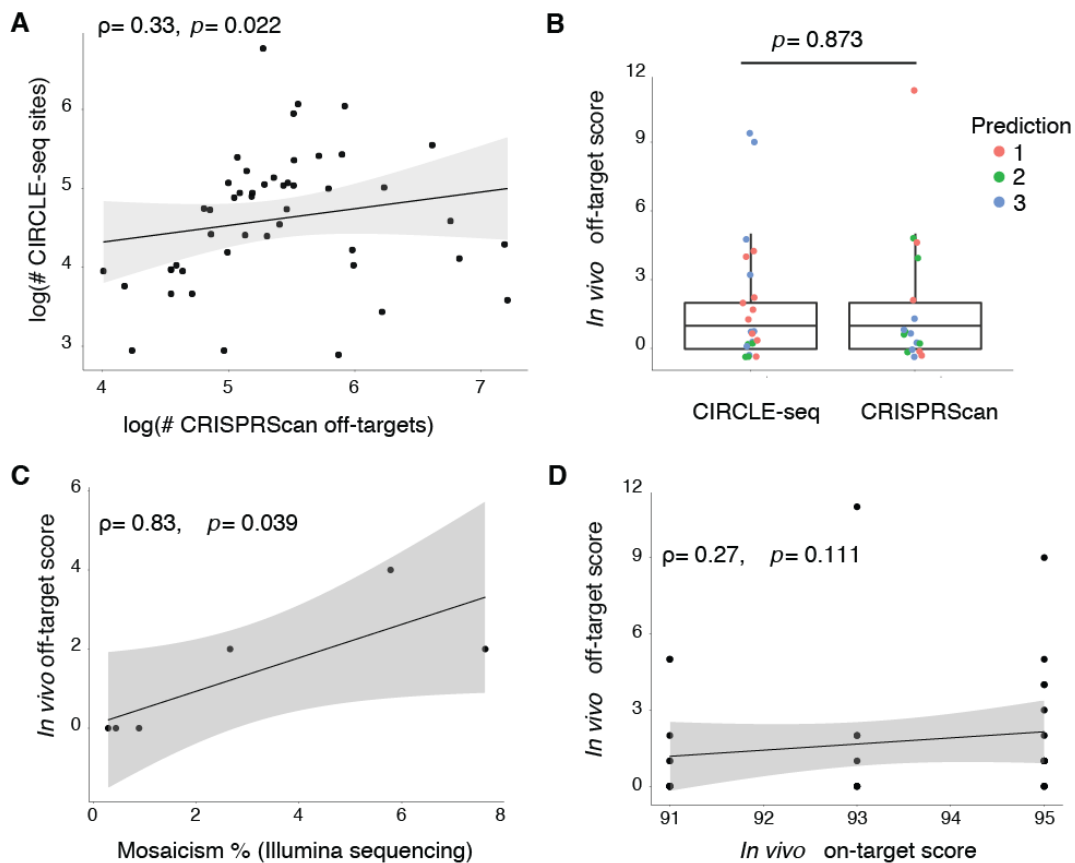
10   **Figure 3. Assessment of off-target cleavage events using different prediction methods. (A)** The number of
11   predicted CRISPRScan off-target sites correlated with the number of identified CIRCLE-seq sites (Spearman
12   correlation). Log normalization was used to reduce the range in the number of sites. **(B)** *In vivo* editing scores from
13   the ICE tool for the top predicted off-target sites using CRISPRScan and CIRCLE-seq were not different. Scores
14   were compared using a Mann-Whitney U test. **(C)** Editing efficiencies at predicted off-target sites using *in vivo*
15   scores from Sanger sequencing and mosaicism % from Illumina sequencing were correlated (Spearman correlation).
16   **(D)** Editing scores obtained *in vivo* at off-target sites were not correlated with the on-target efficiency of the gRNA.
17   All scatter plots include the Spearman correlations results with the line of best fit.
18

1   We also tested if sites predicted with higher likelihoods of off-target cutting events resulted in

2   higher mutation rates by comparing the indel frequencies among the different levels of prediction

3   (top 1, 2, or 3 prediction scores by CRISPRScan or CIRCLE-seq). No differences were found

4   between prediction groups (Kruskal-Wallis: $H_{(2)}= 2.26$, $p= 0.320$; Figure 3B), suggesting that the

5   information used by the tools to assign probabilities of off-target activity (e.g., CFD scores in

6   CRISPRScan or normalized read counts in CIRCLE-seq) do not necessarily predict the

7   efficiency of cutting at off-target sites *in vivo*. Thus, off-target cutting mutations at the assessed

8   sites exhibited low frequencies with no clear method performing best. Moreover, none of the on-

9   target scores previously obtained (*in silico, in vitro*, or *in vivo*) correlated with the number of

10   *predicted* off-target sites per gRNA (using either CRISPRScan or CIRCLE-seq), nor the

11   frequency of indels at validated off-target sites (Spearman $\rho= 0.27$, $p= 0.111$, Figure 3D),

12   suggesting that higher on-target efficiencies do not necessarily translate into increased

13   frequencies of spurious off-target mutations.

14

15   **Evaluating CRISPR Cas9-injection controls**

16   A commonly used 'mock' injection control for phenotypic screens of CRISPR-generated G_0

17   mosaic lines are embryos injected with buffer and Cas9 in the absence of a gRNA. We sought to

18   determine if such control treatments could significantly impact the genome or transcriptome of

19   our zebrafish larvae. To characterize its impact on genes, we performed RNA-seq of wild-type

20   NHGRI-1 embryos injected with either Cas9 enzyme or Cas9 mRNA (three biological replicates

21   of a pool of five injected larvae), uninjected batch siblings (two biological replicates of a pool of

22   five larvae), and uninjected siblings from another batch (three biological replicates with a pool of

23   five larvae) as controls.

1   *Potential genomic mutations in controls*

2   Recently, Sundaresan and colleagues [46] found that Cas9 in the presence of Mn^{+2} ions can

3   result in double-strand cleavage of genomic DNA in the absence of a gRNA. Although their

4   study did not show this same off-target cleavage activity in the presence of Mg^{+2}, we

5   hypothesized that aberrant genomic mutations could be incurred by Cas9 due to the presence of

6    $MgCl_2$ in our injection buffer since Mg^{+2} has been shown to compete with Mn^{+2} in activating

7   common enzymes [47]. Using our RNA-seq data, we used an optimized pipeline [48] to identify

8   somatic mosaic mutations with uninjected wild-type controls as a reference for common

9   polymorphisms. Focusing only on high-confidence variants (minimum sequence read depth of

10   20), we filtered already-reported variants in the NHGRI-1 zebrafish line [49], and used the

11   Variant Effect Predictor tool from ENSEMBL to obtain a list of frameshift mutations in protein-

12   coding genes present in our Cas9-injected larvae. A total of 48 and 38 genes were identified with

13   frameshifting variants in larvae injected with Cas9-enzyme and Cas9-mRNA, respectively, with

14   14 of these genes shared across both injection types (Figure 4A, Supplementary Table 4). On

15   average, each pool of larvae injected with Cas9 enzyme or mRNA carried frameshift variants in

16   18.7±3.1 genes. All identified frameshift variants evidenced low allelic frequencies (Cas9-

17   enzyme: average 0.043, range 0.0036-0.142; Cas9-mRNA: average 0.059, range 0.002-0.316)

18   and high read depth (Cas9-enzyme: average 386.5, range 22-2076; Cas9-mRNA: average 343.8,

19   range 20-3453) (Supplementary Table 4). Additionally, frameshift variants were positioned

20   closer to a potential Cas9 PAM site (NGG) than by random chance (4 bp median observed

21   distance to closest PAM site; empirical $p= 0.0016$ using the whole-genome and $p= 0.006$ using

22   protein-coding regions only, from 10,000 permutations). Therefore, we decided to evaluate if

23   indels would consistently arise in these genes in an additional set of microinjections.

1   We performed a new set of microinjections in NHGRI-1 larvae using these same controls (Cas9

2   enzyme and Cas9 mRNA) and two additional ones commonly used in CRISPR experiments

3   (catalytically dead Cas9 (dCas9) enzyme and a scrambled gRNA coupled with Cas9 enzyme,

4   sequence published in [19]) and evaluated the presence of mutations in 21 genes, including 14

5   genes with identified frameshift mutations in our RNA-seq data and seven controls with no

6   mutations observed (Figure 4B, see Supplementary Table 1 and Supplementary Table 5 for the

7   description of all sites). Briefly, genomic DNA was harvested from (1) three pools of five larvae

8   from each group injected at the one-cell stage (Cas9 enzyme, Cas9 mRNA, dCas9, scrambled

9   gRNA); (2) three pools of five uninjected batch siblings larvae; and (3) finclips of the crossing

10   parents as controls. Subsequently, ~200 bp regions surrounding the closest Cas9 PAM site to the

11   previously RNA-seq-identified variants were Illumina sequenced and the alleles extracted using

12   *CrispRVariants* [50]. We did not observe evidence of inflation of indels in any of the injected

13   groups relative to the uninjected batch siblings or the parental fish, with an overall average

14   mosaicism of 3.1±0.8% per site (below the expected 10% allele ratio for a heterozygous variant

15   in a single individual from a pool of five; Figure 4B, Supplementary Table 5). Our NHGRI-1

16   zebrafish carried common single nucleotide variants in the targeted regions, particularly in gene

17   *si:ch1073-110a20* where two variants were present in close to 50% and 20% of the reads

18   (Supplementary Figure 2). Interestingly, we did observe a subtly higher mosaicism in the genes

19   previously detected with variants in our RNA-seq data relative to the regions used as controls

20   (Mann-Whitney U= 2251.5, *p*= 0.00074, median mosaicism in tested genes 3.4%, median

21   mosaicism in control genes 2.88%; Figure 4B, Supplementary Table 5). Thus, it is possible that

22   the genes we identified with variants in our RNA-seq data may be naturally prone to carry

23   variants. In summary, these results suggest that currently used CRISPR controls do not suffer

1   systematic DNA cleavages in the absence of a gRNA.

2
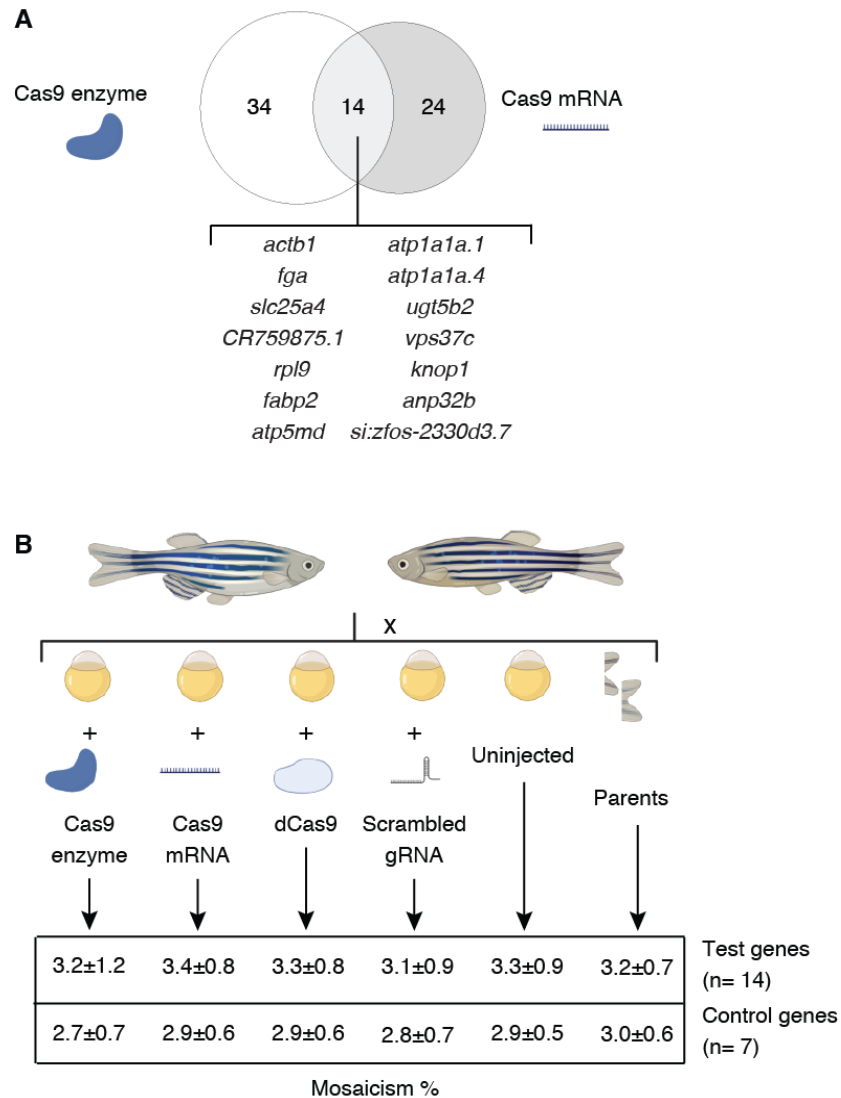
Figure 4. Evaluation of spurious genomic mutations in CRISPR-injection controls. (A) The abundance of protein-coding genes carrying frameshift variants for each Cas9-injected treatment are depicted in a Venn diagram, with mutated genes identified in both treatments listed. **(B)** Genomic DNA from zebrafish larvae injected with Cas9 enzyme, Cas9 mRNA, catalytically dead Cas9 (dCas9), a scrambled gRNA, uninjected batch siblings, and a fin clip from their parents was used to perform targeted Illumina sequencing of 21 genes to quantify indel mosaicism with average ± standard deviation values listed in the table (see Supplementary Table 1 and Supplementary Table 7 for the description of the genes).

11

12   *Differential gene expression in controls*

13   We also characterized the impact of injecting Cas9 enzyme or mRNA on the transcriptomes of

14   our zebrafish larvae. Comparisons of transcripts abundances show significant variance across

1   biological replicates when quantifying in both Cas9 treatments, particularly evident in samples

2   injected with the Cas9 enzyme, versus wild-type uninjected larvae (Figure 5A). This suggests

3   that considerable stochasticity may exist regarding the effects of Cas9 injections in these

4   controls. Examining the genes impacted, we identified hundreds of differentially-expressed (DE)

5   genes in our Cas9-injected versus uninjected controls, with a greater number of upregulated

6   genes than downregulated genes (Figure 5B, Supplementary Table 6). Specifically, Cas9-enzyme

7   injections resulted in a total of 1,100 DE genes (3.6% of the genes assayed), with 756 genes

8   (68.7%) upregulated (fold change > 1) and 344 (31.3%) downregulated (fold change < -1). Cas9-

9   mRNA injected larvae exhibited 548 DE genes (1.8% of the genes assayed), 376 (68.6%) of

10   these upregulated and 172 (31.4%) downregulated (Figure 5B). We observed 248 (197

11   upregulated and 51 downregulated) common DE genes between the two treatments (Figure 5C),

12   which could be part of a common response to the microinjection process. Network analyses

13   identified commonalities in the shared DE genes enriched in key regulators of different KEGG

14   pathways, including spliceosome and ribosome (including genes *eif4g2b*, *eif4g1a*, *hnrnpd*,

15   *magoh*, *hnrnpa0a*), hedgehog signaling (*shha*), glutathione metabolism (*gsto2*, *gsr*), GnRH

16   signaling (*dusp6*), aminoacyl-tRNA biosynthesis (*yars*), cell cycle (*kif2c*), glycolysis (*aldoca*),

17   and cellular senescence (*ppp3cca*) (Supplementary Figure 3). Furthermore, while we observed

18   no enrichment in gene ontology terms for downregulated genes, common upregulated genes

19   from both treatments were related to response to wounding (GO:0009611, adjusted *p*-value=

20   0.009) and cytoskeleton organization (GO:0045104, adjusted *p*-value=0.009) (Supplementary

21   Table 7), revealing molecular consequences of the microinjection process that were still

22   detectable five days later.
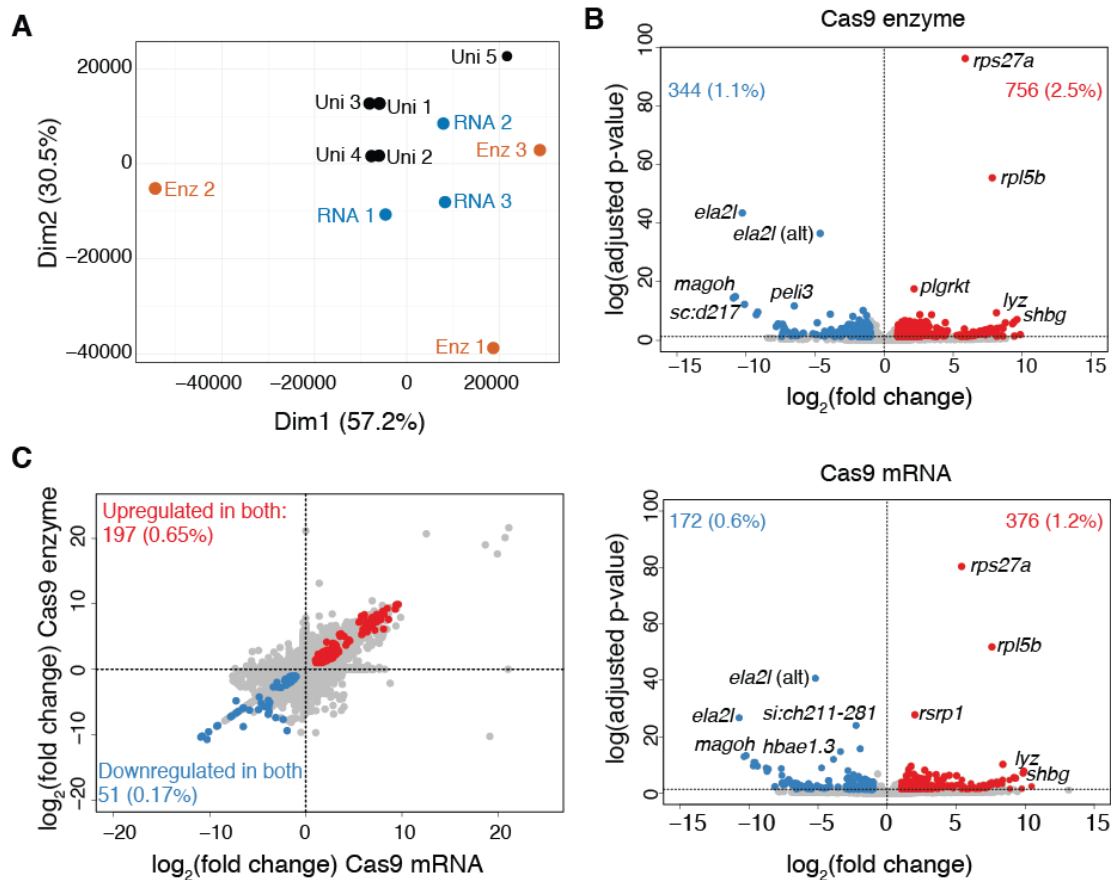
Figure 5. Evaluation of expression variability in CRISPR-injection controls. (A) Principal components analysis using the transcript abundances in larvae injected with Cas9 enzyme (Enz1, Enz2, Enz3), Cas9 mRNA (RNA1, RNA2, RNA3), uninjected siblings (Uni1, Uni2), and uninjected siblings from a different batch (Uni3, Uni4, Uni5). **(B)** Volcano plots show the differentially-expressed genes in Cas9-enzyme and Cas9-mRNA injected larvae with the number (and %) of upregulated (fold change > 1) and downregulated (fold change < -1) genes. The top five representative up- and downregulated genes are highlighted, with the full list of genes available as Supplementary Table 6. **(C)** Differentially-expressed genes across samples injected with Cas9 enzyme or Cas9 mRNA relative to uninjected batch-siblings show significant correlations. Plots include the numbers and percentages (in parentheses) of genes downregulated (blue) and upregulated (red) in both Cas9 treatments from the total amount of genes assayed (n= 30,258).

DISCUSSION

Our study presents a comprehensive evaluation of empirical and predictive tools currently used for CRISPR editing in zebrafish. Cleavage scores obtained by an *in vivo* assessment of 50 gRNAs via Sanger sequencing and deconvolution tools (ICE and TIDE) were concordant with Illumina sequencing, the gold standard in predicting efficiencies, as previously reported [34]. Both tools underestimated the presence of non-edited alleles by ~20%, contrary to previous

1   comparisons of TIDE and Illumina sequencing in cell lines, where TIDE showed a ~10–20%

2   overestimation of non-edited alleles [51]. For sites with lower indel frequencies, as we observed

3   for predicted off-target mutations, ICE scores were more concordant with Illumina results (~1–

4   2% difference, again mostly underestimates). Therefore, we suggest that Sanger sequencing

5   deconvolution tools are valuable for establishing relative gRNAs efficiencies but do not

6   necessarily accurately predict absolute cleavage efficiencies in zebrafish *in vivo*, except at sites

7   with low indel frequencies. In addition, we formalized an empirical 'intensity ratio' score from

8   the commonly-used PAGE approach to assay CRISPR indels and verified its utility in

9   approximating cleavage efficiencies, making it a more affordable and rapid approach to assay

10 editing efficiencies versus sequencing.

11

12 On-target efficiency prediction tools showed large differences using the same set of gRNAs

13 sequences, highlighting the importance of understanding features accounted for by each tool. A

14 recent review [25] provides a comprehensive overview of different design tools available and the

15 source of experimental data used to train each one. CRISPRScan [26] was the only tool that

16 could predict on-target efficiency in our set of gRNAs, while no other method provided scores

17 that were correlated with cleavage activities observed *in vivo*. One limitation of our study was

18 the skew in higher efficiency gRNAs (mean predicted CRISPRScan score of 57.6), which could

19 feasibly impact correlations. Notably, we did obtain more accurate CRISPRScan predictions

20 when we utilized our NHGRIzed reference [49] compared to the current Tübingen-derived

21 reference [4], highlighting the importance of accounting for known genetic variation when

22 designing suitable gRNAs [52, 53]. Considering CRISPRScan was the only tool that

23 incorporated empirical data from zebrafish, with most methods tested using *in vitro*-derived data,

1   our results emphasize the importance of utilizing a tool trained using *in vivo* experimental data

2   specific to the study's target species.

3

4   An *in silico* (CRISPRScan) and *in vitro* (CIRCLE-seq) method predicted ~20% and 65%

5   potential off-target regions impacting genes, respectively. Notably, we did not evaluate if other

6   predicted sites included *cis*-regulatory elements that could also potentially alter gene expression.

7   Future assessments should include tests targeting a diversity of loci for a more thorough

8   understanding of the potential off-target indels caused by unwanted CRISPR cleavage sites. We

9   observed low off-target mutation frequencies (most <1%), similar to those previously reported

10   from using single [11, 12] or multiple gRNAs [18], although did observe off-target indel

11   frequencies as high as 11% for certain gRNAs. Notably, neither predictive method (CRISPRScan

12   or CIRCLE-seq) nor their likelihood score (using CFD or normalized read count) could

13   accurately predict indel frequencies at off-target sites. Typically, such low mutation frequencies

14   should not be of high impact when generating stable knockout zebrafish lines as these could be

15   easily outcrossed. However, such mutations could have significant impacts on phenotypic

16   outcomes when injected G_0 mosaic populations are analyzed directly.

17

18   The adequate selection of controls is a fundamental process in evaluating gene function using G_0

19   knockout crispant zebrafish, as these larvae serve as baselines from which inferences will be

20   made from. Currently, no consensus exists for preferred controls used in high-throughput

21   CRISPR workflows of zebrafish larvae, which can include targeting a known gene as a positive

22   control (e.g., *tyr*) [14], uninjected larvae [17, 18], sham injections with a Cas9:tracrRNA

23   complex [15], and injections of a scrambled gRNA [16, 19], among others. Our RNA-seq assay

1   identified several genes carrying frameshift mutations using uninjected clutch siblings as

2   reference. A follow-up analysis of a second set of injections showed existence of mosaic variants

3   in all injected controls (e.g., Cas9 mRNA, enzyme, and scrambled gRNA), in addition to

4   uninjected siblings and crossed parents at low allelic frequencies (~3%). Nevertheless, even

5   though we were limited to our targeted regions, we did observe a higher mosaicism in genes

6   identified as carrying frameshift mutations from our RNA-seq assay compared to control genes,

7   suggesting that these genes could be naturally prone to exhibit mutations in the NHGRI-1

8   zebrafish line. We also observed high variability in gene expression in larvae solely injected with

9   Cas9 enzyme or mRNA, with several of these DE genes involved in response to wounding

10   processes. Notably, these DE genes were retrieved from 5 dpf larvae suggesting that damage

11   incurred during the microinjection process has a lasting effect. These results suggest that caution

12   should be taken in using G_0 mosaic mutants in investigating phenotypes related to pathways

13   found to be significantly skewed in injection controls, including those involving the function of

14   the spliceosome, ribosomes, and cytoskeleton dynamics.

15

16   **CONCLUSIONS**

17   Overall, we performed a simultaneous assessment of gRNA activities predicted by several

18   commonly used *in silico* and *in vitro* methods with those determined experimentally *in vivo* in

19   injected zebrafish embryos. These results provide valuable information that can be incorporated

20   into the design and execution of CRISPR/Cas9 assays in zebrafish using available workflows [8,

21   13, 14, 17, 18]. Namely, we make the following conclusions and recommendations:

- Sanger-based efficiency estimates (TIDE and ICE) tend to underestimate indel mosaicism in zebrafish, though they are more accurate when lower mutational mosaicism exists (such as those observed at off-target sites).
- Quantifying heterodimers via PAGE gels represents an affordable method to qualitatively assay CRISPR cutting efficiencies.
- Of the existing tools, we recommend CRISPRScan for predicting gRNA on-target efficiency, preferably matched to the zebrafish strain being used.
- Off-target mutations occur at relatively low rates with neither *in silico* nor *in vitro* prediction methods performing significantly better.
- Microinjection of Cas9 (enzymes or mRNA) into embryos does not result in spurious genomic mutations but does impact certain genes and pathways. Caution should be exercised if studying phenotypes related to these genes when performing G_0 mosaic zebrafish screens.

Our aim was to provide information to aid in the decision-making process for future projects using affordable and reliable gene-editing tools in zebrafish. As higher-throughput methods continue to be developed for assaying multiple genes simultaneously, it will be important to use optimal tools for predicting and assessing on- and off-target activity in zebrafish larvae for accurate interpretation of phenotypic outcomes.

METHODS

Zebrafish husbandry

1   NHGRI-1 wild-type zebrafish [49] were maintained through standard protocols [54] and their

2   use was approved by the Institutional Animal Care and Use Committee from the Office of

3   Animal Welfare Assurance, University of California, Davis. Animals were kept in a temperature

4   (28±0.5°C) and light (10 h dark/14 h light cycle) controlled modular system with UV-sterilized

5   filtered water (Aquaneering, San Diego, CA), with a density of 25 adult fish per tank. Feeding

6   and general monitoring of all zebrafish was performed twice a day (9 am and 4 pm). Food

7   included rotifers (Rotigrow Nanno, Reed Mariculture, Campbell, CA), brine shrimp (Artemia

8   Brine Shrimp 90% hatch, Aquaneering, San Diego, CA), and flakes (Zebrafish Select Diet,

9   Aquaneering, San Diego, CA). For all experimental procedures, eggs were collected via natural

10   spawning of randomly selected adult NHGRI-1 zebrafish in 1 liter crossing tanks (Aquaneering,

11   San Diego, CA), using a minimum of five breeding pairs (1 male, 1 female) unless otherwise

12   specified. Embryos were grown in standard Petri dishes with E3 media (0.03% Instant Ocean salt

13   in deionized water) and incubated at 28±0.5°C, using a dissecting microscope (Leica, Buffalo

14   Grove, IL) for developmental staging and daily monitoring until their use for molecular

15   procedures.

16

17   **Design and *in silico* predictions for gRNAs**

18   50 gRNAs targeting exons of 14 genes were designed using CRISPRScan [26] (scores ranging

19   between 24 and 83 with a mean value of 57.6) with zebrafish genome version GRCz11/danRer11

20   as the reference (see description of gRNAs in Supplementary Tables 1 and 2). All targeted genes

21   were protein coding. For each designed gRNA, we obtained the efficiency scores predicted by

22   CRISPRScan [26], CHOPCHOP [35–37] using the scoring method from [38] and [39], E-CRISP

23   [40], CRISPR-GE [41], CCTop [42], CRISPRon [43], DeepSpCas9 [44], and the IDT design tool

1   (www.idtdna.com). From CRISPRScan, we also gathered the predicted off-target sites for each

2   gRNA defined by the CFD score [26]. Additionally, we utilized *bedtools* [55] to determine the

3   GC percentage for each gRNA. To incorporate NHGRI-1 variants into the zebrafish reference,

4   we used the FastaAlternateReferenceMaker function from *GATK* [56] with the reported high-

5   confidence variants for the NHGRI-1 zebrafish strain [49].

6

7   **Microinjections to generate CRISPR G_0 mosaic mutants**

8   All gRNAs were individually injected into NHGRI-1 embryos to estimate the frequency of

9   indels. gRNAs were prepared following the manufacturer's protocol (Integrated DNA

10   Technologies). Briefly, 2.5 μl of 100 μM crRNA, 2.5 μl of 100 μM tracrRNA, and 5 μl of

11   Nuclease-free Duplex Buffer using an annealing program consisting of 5 min at 95°C, a ramp

12   from 95°C to 50°C with a -0.1°C/s change, 10 minutes (min) at 50°C, and a ramp from 50°C to

13   4°C with a -1°C/s change. Ribonucleoprotein injection mix was prepared with 1.30 μl of Cas9

14   enzyme (20 μM, New England BioLabs), 1.60 μl of prepared gRNAs, 2.5 μl of 4x Injection

15   Buffer (containing 0.2% phenol red, 800 mM KCl, 4 mM $MgCl_2$, 4 mM TCEP, 120 mM HEPES,

16   pH 7.0), and 4.6 μl of Nuclease-free water. Microinjections directly into the yolk of NHGRI-1

17   embryos at the one-cell stage were performed as described previously [57], using needles from a

18   micropipette puller (Model P-97, Sutter Instruments) and an air injector (Pneumatic MPPI-2

19   Pressure Injector). Embryos were collected and ~1 nl of ribonucleoprotein mix was injected per

20   embryo, after previous calibration with a microruler. Twenty injected embryos per Petri dish

21   were grown up to 5 dpf at 28°C.

22

23   **Illumina and Sanger amplicon sequencing**

1   DNA extractions were performed on 20 pooled embryos by adding 100 μl of 50 mM NaOH,

2   incubation at 95°C for 20 min, ramp from 95°C to 4°C at a 0.7°C/s decrease, followed by an

3   addition of 10 μl of 1 M Tris-HCl and a 15 min spin at 4680 rpm. We amplified a ~200 bp region

4   surrounding the targeted site of each gRNA (see Supplementary Table 1 for description of

5   primers). PCR amplifications were performed using 12.5 μl of 2X DreamTaq Green PCR Master

6   Mix (Thermo Fisher), 9.5 μl of Nuclease-Free water, 1 μl of 10 μM primers, and 1 μl extracted

7   DNA. Thermocycler program included 3 min at 95°C, followed by 35 cycles of 15 s at 95°C, 30

8   s at 60°C, and 20 s at 72°C, and a final 5 min incubation at 72°C. Reactions were purified using

9   Ampure XP magnetic beads (Beckman Coulter) and Illumina sequenced (Genewiz, San Diego,

10   CA). To obtain percent mosaicism of mutants by mapping paired-end fastq reads to the zebrafish

11   reference genome (GRCz11/danRer11) using *bwa* [57] and the R package *CrispRVariants* [35].

12   Additionally, we amplified a ~500 bp region surrounding the targeted site of each gRNA from

13   the same extracted DNA for six gRNAs and performed and performed Sanger sequencing

14   (Genewiz, San Diego, CA). Raw trace files were used in the TIDE [33] and ICE [34] tools to

15   predict the percentage of indels, which we used as our *in vivo* editing score for each gRNA. For

16   both Sanger and Illumina sequencing, we used uninjected batch-sibling embryos as a control

17   reference.

18

19   **PAGE and intensity-ratio estimation**

20   An empirical cleavage analysis from each gRNA was performed using PAGE. Briefly, we

21   amplified a ~200 bp region in DNA around the targeted site from gRNA-injected and uninjected

22   embryos, as described above. Reactions of the uninjected and injected samples from the same

23   amplicon were run on a 7.5% polyacrylamide gel together for 75 min at 110 V and revealed

1   using GelRed (VWR International). Gel images were processed in the software Fiji [58]. For

2   each sample, we defined areas **A** and **B** as follows:
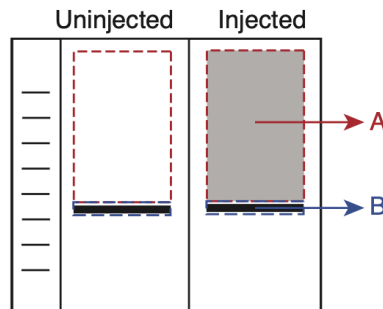
3

4   For each gRNA, the mean-intensity value was obtained for the A and B areas in both the injected

5   and uninjected samples. The A and B areas were exactly the same size between samples. The

6   intensity ratio was calculated as: [injected B / injected A] / [uninjected B / uninjected A]. Log-

7   normalized intensity ratios followed a normal distribution (Shapiro-Wilk test: W= 0.96, $p=$

8   0.167) with an average value of 1.21±0.70.

9

10 **CIRCLE-seq**

11 CIRCLE-seq libraries were prepared for each gRNA (IDT) using genomic DNA extracted from

12 NHGRI-1 (DNA Blood & Tissue kit, Qiagen) following the described protocol [59]. Libraries

13 were sequenced using one HiSeq XTen lane (Novogene, Sacramento, CA), providing an average

14 of 7.3 million reads (range: 4.0 - 13.3 million reads) and >Q30 for 92% of reads per gRNA

15 library. Raw reads were processed using the bioinformatic pipeline described [59] (mapping rate

16 >99% in all samples) to identify regions with cutting events relative to a control sample (treated

17 with Cas9 enzyme and no gRNA). In an attempt to obtain an on-target efficiency estimation from

18 *in vitro* digestions, we calculated the reads per million normalized (RPMN). For this purpose, we

19 used *samtools* [60] to extract read coverage from aligned bam files. For each gRNA, coverage

1   was obtained for the third and fourth base upstream of the PAM site as it is the region expected

2   to be cut by Cas9 [61]. RPMN for each gRNA was calculated as the sum of coverage at these

3   two sites divided by the total mapped reads per sample and multiplied by one million to scale the

4   values. RPMN scores ranged from 4.42 to 881 (median 99.3) so we decided to use a log

5   normalization to reduce this range.

6

7   **RNA-seq**

8   We performed RNA-seq of Cas9 injected NHGRI-1 larvae to identify potential gRNA-

9   independent cleavage sites. One-cell stage NHGRI-1 embryos were injected with either Cas9

10   enzyme or Cas9 mRNA. Injection mix for Cas9 enzyme included Cas9 enzyme (20 µM, New

11   England BioLabs), 2.5 µl of 4x Injection Buffer (0.2% phenol red, 800 mM KCl, 4 mM MgCl$_2$, 4

12   mM TCEP, 120 mM HEPES, pH 7.0), and Nuclease-free water. Cas9 mRNA was obtained from

13   plasmid pT3TS-nCas9n (Addgene, plasmid #46757) [5], using the MEGAshotscript T3

14   transcription kit (Thermo Fisher) following manufacturer's guidelines of 3.5 h 56°C incubation

15   with T3. mRNA was purified with the MEGAclear transcription clean-up kit (Thermo Fisher)

16   and concentration of mRNA obtained using a NanoDrop (Thermo Fisher). The injection mix of

17   Cas9 mRNA contained 100 ng/µl of mRNA, 4x Injection Buffer (0.2% phenol red, 800 mM

18   KCl, 4 mM MgCl$_2$, 4 mM TCEP, 120 mM HEPES, pH 7.0), and Nuclease-free water.

19   Additionally, uninjected batch-siblings and uninjected siblings from an additional batch were

20   used as controls. All embryos were grown at 28°C in a density of <50 embryos per dish. At 5

21   dpf, three pools of five larvae were collected for each group (Cas9 enzyme, Cas9 mRNA, and

22   uninjected) for RNA extraction using the RNeasy kit (Qiagen) with genomic DNA eliminator

1   columns for DNA removal. Whole RNA samples were subjected to RNA-seq using the poly-A

2   selection method (Genewiz, San Diego, CA).

3

4   **Variant identification from RNA-seq data**

5   We followed a previously described pipeline to identify somatic variants from RNA-seq data

6   [48]. Briefly, we mapped reads with *STAR* [62] using the 2-pass mode and a genomic reference

7   created with GRCz11/danRer11 assembly and gtf files (release version 100). Variant calling was

8   performed with MuTect2 as part of *GATK* [56] using the tumor versus normal mode. 'Normal'

9   was defined by the two uninjected samples to identify all somatic mutations in our Cas9 injected

10   embryos. Variants were annotated using the Variant Effect Predictor tool [63]. High confidence

11   variants (minimum sequencing depth of 20) previously reported for the NHGRI-1 line [49] were

12   removed. Only frameshift loss-of-function variants with a minimum read depth of 20 in

13   canonical protein-coding genes were considered. We extracted the median distance between the

14   identified variants and the nearest Cas9 PAM site (NGG sequence) using the coordinates in the

15   CRISPRScan UCSC track. This median observed distance was compared to the result of median

16   distances of 10,000 permutations of random sampling across the genome and their nearest PAM

17   site. One-tailed empirical *p* values from this comparison were calculated as (M+N)/(N+1), where

18   M is the number of iterations with a median distance below the observed value and N is the total

19   number of iterations. We orthogonally investigated the presence of variants in 23 genes via

20   Illumina sequencing of a ~200 bp region surrounding the identified variant location and the R

21   package *CrispRVariants* [50] (Supplementary Table 1 for primers description). For this purpose,

22   we extracted DNA from 3 pools of 5 embryos injected with Cas9 enzyme, Cas9 mRNA, dCas9

23   (Alt-R S. p. dCas9 protein V3 from IDT), a scrambled gRNA (see Supplementary Table 1 for

sequence description), or uninjected. In addition, we extracted DNA from a finclip of the

crossing parents of the embryos used for the injections (both female and male). In all of these

groups, we quantified the percentage of mutations as all alleles different from the reference.

Differential gene expression analysis from RNA-seq data

Raw reads were processed using the *elvers* (https://github.com/dib-lab/elvers; version 0.1,

release DOI: 10.5281/zenodo.3345045) bioinformatic pipeline that utilizes *fastqc* [64],

trimmomatic [65], and *salmon* [66] to obtain the transcripts per kilobase million (TPM) for each

gene. *DESeq2* [67] was used to extract differentially-expressed genes in the Cas9 enzyme or

Cas9 mRNA injected samples relative to the uninjected larvae. R package *clusterProfiler* [68]

was used to perform enrichment tests of differentially-expressed genes in biological pathways.

Network analyses of the common differential expressed genes was performed using the

NetworkAnalyst online tool (www.networkanalyst.ca) [69, 70].

Statistical analyses

All analyses were performed in R version 4.0.2 [71]. Normality of variables was checked using

the Shapiro-Wilk test and parametric or nonparametric comparisons made accordingly.

Spearman correlation tests (denoted as ρ) and linear regression models were used to determine

the relationship between variables. All analyses compared across different experimental batches

included *batch* as a factor in the model to prevent biases caused by inter-batch differences.

Averages include the standard deviation unless otherwise specified. Alpha to determine

significance across the different tests was set at 0.05 unless otherwise specified. Additional R

packages used for making figures included *eulerr* [72] and pheatmap [73].

1

Abbreviations

3 CFD: cutting frequency determination; CRISPR: clustered regularly interspaced short

4 palindromic repeats; gRNA: guide RNA; indels: insertions or deletions; PAGE: polyacrylamide

5 gel electrophoresis; RPMN: reads per million normalized.

6

DECLARATIONS

Ethics approval and consent to participate

9 Animal use was approved by the University of California, Davis Institutional Animal Care and

10 Use Committee (IACUC) from the Office of Animal Welfare Assurance accredited by the

11 Association for Assessment and Accreditation of Laboratory Animal Care (Assurance Number

12 A3433-01 on file with the Office of Laboratory Animal Welfare). The IACUC is constituted in

13 accordance with U.S. Public Health Service Animal Welfare Policy and includes a member of

14 the public and a non-scientist. The study and all methods were carried out in accordance with

15 relevant guidelines and regulations and in compliance with the ARRIVE guidelines [74].

16

Consent for publication

18 Not applicable.

19

Availability of data and materials

21 Original fastq files from the CIRCLE-seq and RNA-seq assays are deposited in the European

22 Nucleotide Archive repository under project PRJEB39643.

23

1   of this manuscript for their helpful comments and suggestions that have significantly improved

2   our study.

3

4   **REFERENCES**

5   1. Meyers JR. Zebrafish: Development of a Vertebrate Model Organism: Zebrafish :
6   Development of a Vertebrate Model Organism. Current Protocols Essential Laboratory
7   Techniques. 2018;16:e19.

8   2. Holtzman NG, Iovine MK, Liang JO, Morris J. Learning to Fish with Genetics: A Primer on
9   the Vertebrate Model Danio rerio. Genetics. 2016;203:1069–89.

10   3. Liu J, Zhou Y, Qi X, Chen J, Chen W, Qiu G, et al. CRISPR/Cas9 in zebrafish: an efficient
11   combination for human genetic diseases modeling. Hum Genet. 2017;136:1–12.

12   4. Howe K, Clark MD, Torroja CF, Torrance J, Berthelot C, Muffato M, et al. The zebrafish
13   reference genome sequence and its relationship to the human genome. Nature. 2013;496:498–
14   503.

15   5. Jao L-E, Wente SR, Chen W. Efficient multiplex biallelic zebrafish genome editing using a
16   CRISPR nuclease system. Proc Natl Acad Sci U S A. 2013;110:13904–9.

17   6. Hwang WY, Fu Y, Reyon D, Maeder ML, Tsai SQ, Sander JD, et al. Efficient genome editing
18   in zebrafish using a CRISPR-Cas system. Nat Biotechnol. 2013;31:227–9.

19   7. Irion U, Krauss J, Nüsslein-Volhard C. Precise and efficient genome editing in zebrafish using
20   the CRISPR/Cas9 system. Development. 2014;141:4827–30.

21   8. Varshney GK, Pei W, LaFave MC, Idol J, Xu L, Gallardo V, et al. High-throughput gene
22   targeting and phenotyping in zebrafish using CRISPR/Cas9. Genome Res. 2015;25:1030–42.

23   9. Vejnar CE, Moreno-Mateos MA, Cifuentes D, Bazzini AA, Giraldez AJ. Optimized CRISPR-
24   Cas9 System for Genome Editing in Zebrafish. Cold Spring Harb Protoc. 2016;2016.
25   doi:10.1101/pdb.prot086850.

26   10. Chang N, Sun C, Gao L, Zhu D, Xu X, Zhu X, et al. Genome editing with RNA-guided Cas9
27   nuclease in zebrafish embryos. Cell Res. 2013;23:465–72.

28   11. Hruscha A, Krawitz P, Rechenberg A, Heinrich V, Hecht J, Haass C, et al. Efficient
29   CRISPR/Cas9 genome editing with low off-target effects in zebrafish. Development.
30   2013;140:4982–7.

31   12. Burger A, Lindsay H, Felker A, Hess C, Anders C, Chiavacci E, et al. Maximizing
32   mutagenesis with solubilized CRISPR-Cas9 ribonucleoprotein complexes. Development.

1   2016;143:2025–37.

2   13. Gagnon JA, Valen E, Thyme SB, Huang P, Akhmetova L, Pauli A, et al. Efficient
3   mutagenesis by Cas9 protein-mediated oligonucleotide insertion and large-scale assessment of
4   single-guide RNAs. PLoS One. 2014;9:e98186.

5   14. Varshney GK, Carrington B, Pei W, Bishop K, Chen Z, Fan C, et al. A high-throughput
6   functional genomics workflow based on CRISPR/Cas9-mediated targeted mutagenesis in
7   zebrafish. Nat Protoc. 2016;11:2357–75.

8   15. Watson CJ, Monstad-Rios AT, Bhimani RM, Gistelinck C, Willaert A, Coucke P, et al.
9   Phenomics-Based Quantification of CRISPR-Induced Mosaicism in Zebrafish. Cell Syst.
10   2020;10:275–86.e5.

11   16. Wu RS, Lam II, Clay H, Duong DN, Deo RC, Coughlin SR. A Rapid Method for Directed
12   Gene Knockout for Screening in G0 Zebrafish. Dev Cell. 2018;46:112–25.e4.

13   17. Hoshijima K, Jurynec MJ, Klatt Shaw D, Jacobi AM, Behlke MA, Grunwald DJ. Highly
14   Efficient CRISPR-Cas9-Based Methods for Generating Deletion Mutations and F0 Embryos that
15   Lack Gene Function in Zebrafish. Dev Cell. 2019;51:645–57.e4.

16   18. Shah AN, Davey CF, Whitebirch AC, Miller AC, Moens CB. Rapid Reverse Genetic
17   Screening Using CRISPR in Zebrafish. Nature Methods. 2015;12:152–3.

18   19. Kroll F, Powell GT, Ghosh M, Gestri G, Antinucci P, Hearn TJ, et al. A simple and effective
19   F0 knockout method for rapid screening of behaviour and other complex phenotypes. Elife.
20   2021;10. doi:10.7554/eLife.59683.

21   20. Thyme SB, Pieper LM, Li EH, Pandey S, Wang Y, Morris NS, et al. Phenotypic Landscape
22   of Schizophrenia-Associated Genes Defines Candidates and Their Shared Functions. Cell.
23   2019;177:478–91.e20.

24   21. Liu K, Petree C, Requena T, Varshney P, Varshney GK. Expanding the CRISPR Toolbox in
25   Zebrafish for Studying Development and Disease. Front Cell Dev Biol. 2019;7:13.

26   22. Zischewski J, Fischer R, Bortesi L. Detection of on-target and off-target mutations generated
27   by CRISPR/Cas9 and other sequence-specific nucleases. Biotechnol Adv. 2017;35:95–104.

28   23. Zhu X, Xu Y, Yu S, Lu L, Ding M, Cheng J, et al. An efficient genotyping method for
29   genome-modified animals and human cells generated with CRISPR/Cas9 system. Sci Rep.
30   2014;4:6420.

31   24. Brocal I, White RJ, Dooley CM, Carruthers SN, Clark R, Hall A, et al. Efficient
32   identification of CRISPR/Cas9-induced insertions/deletions by direct germline screening in
33   zebrafish. BMC Genomics. 2016;17:259.

34   25. Liu G, Zhang Y, Zhang T. Computational approaches for effective CRISPR guide RNA
35   design and evaluation. Comput Struct Biotechnol J. 2020;18:35–44.

1   26. Moreno-Mateos MA, Vejnar CE, Beaudoin J-D, Fernandez JP, Mis EK, Khokha MK, et al.
2   CRISPRscan: designing highly efficient sgRNAs for CRISPR-Cas9 targeting in vivo. Nat
3   Methods. 2015;12:982–8.

4   27. Bao XR, Pan Y, Lee CM, Davis TH, Bao G. Tools for experimental and computational
5   analyses of off-target editing by programmable nucleases. Nat Protoc. 2021;16:10–26.

6   28. Tsai SQ, Nguyen NT, Malagon-Lopez J, Topkar VV, Aryee MJ, Joung JK. CIRCLE-seq: a
7   highly sensitive in vitro screen for genome-wide CRISPR-Cas9 nuclease off-targets. Nat
8   Methods. 2017;14:607–14.

9   29. Tsai SQ, Zheng Z, Nguyen NT, Liebers M, Topkar VV, Thapar V, et al. GUIDE-seq enables
10   genome-wide profiling of off-target cleavage by CRISPR-Cas nucleases. Nat Biotechnol.
11   2015;33:187–97.

12   30. Mooney MR, Davis EE, Katsanis N. Analysis of Single Nucleotide Variants in CRISPR-
13   Cas9 Edited Zebrafish Exomes Shows No Evidence of Off-Target Inflation. Front Genet.
14   2019;10:949.

15   31. Iyer V, Boroviak K, Thomas M, Doe B, Riva L, Ryder E, et al. No unexpected CRISPR-
16   Cas9 off-target activity revealed by trio sequencing of gene-edited mice. PLoS Genet.
17   2018;14:e1007503.

18   32. Dong Y, Li H, Zhao L, Koopman P, Zhang F, Huang JX. Genome-Wide Off-Target Analysis
19   in CRISPR-Cas9 Modified Mice and Their Offspring. G3 . 2019;9:3645–51.

20   33. Brinkman EK, Chen T, Amendola M, van Steensel B. Easy quantitative assessment of
21   genome editing by sequence trace decomposition. Nucleic Acids Res. 2014;42:e168.

22   34. Hsiau T, Conant D, Rossi N, Maures T, Waite K, Yang J, et al. Inference of CRISPR Edits
23   from Sanger Trace Data. doi:10.1101/251082.

24   35. Montague TG, Cruz JM, Gagnon JA, Church GM, Valen E. CHOPCHOP: a CRISPR/Cas9
25   and TALEN web tool for genome editing. Nucleic Acids Res. 2014;42 Web Server issue:W401–
26   7.

27   36. Labun K, Montague TG, Krause M, Torres Cleuren YN, Tjeldnes H, Valen E. CHOPCHOP
28   v3: expanding the CRISPR web toolbox beyond genome editing. Nucleic Acids Res.
29   2019;47:W171–4.

30   37. Labun K, Montague TG, Gagnon JA, Thyme SB, Valen E. CHOPCHOP v2: a web tool for
31   the next generation of CRISPR genome engineering. Nucleic Acids Res. 2016;44:W272–6.

32   38. Doench JG, Fusi N, Sullender M, Hegde M, Vaimberg EW, Donovan KF, et al. Optimized
33   sgRNA design to maximize activity and minimize off-target effects of CRISPR-Cas9. Nat
34   Biotechnol. 2016;34:184–91.

35   39. Xu H, Xiao T, Chen C-H, Li W, Meyer CA, Wu Q, et al. Sequence determinants of improved

CRISPR sgRNA design. Genome Res. 2015;25:1147–57.

40. Heigwer F, Kerr G, Boutros M. E-CRISP: fast CRISPR target site identification. Nat Methods. 2014;11:122–3.

41. Xie X, Ma X, Zhu Q, Zeng D, Li G, Liu Y-G. CRISPR-GE: A Convenient Software Toolkit for CRISPR-Based Genome Editing. Mol Plant. 2017;10:1246–9.

42. Stemmer M, Thumberger T, Del Sol Keyer M, Wittbrodt J, Mateo JL. CCTop: An Intuitive, Flexible and Reliable CRISPR/Cas9 Target Prediction Tool. PLoS One. 2015;10:e0124633.

43. Xiang X, Corsi GI, Anthon C, Qu K, Pan X, Liang X, et al. Enhancing CRISPR-Cas9 gRNA efficiency prediction by data integration and deep learning. Nat Commun. 2021;12:3238.

44. Kim HK, Kim Y, Lee S, Min S, Bae JY, Choi JW, et al. SpCas9 activity prediction by DeepSpCas9, a deep learning–based model with high generalization performance. Science Advances. 2019;5:eaax9249. doi:10.1126/sciadv.aax9249.

45. Chung C-H, Allen AG, Sullivan NT, Atkins A, Nonnemacher MR, Wigdahl B, et al. Computational Analysis Concerning the Impact of DNA Accessibility on CRISPR-Cas9 Cleavage Efficiency. Mol Ther. 2020;28:19–28.

46. Sundaresan R, Parameshwaran HP, Yogesha SD, Keilbarth MW, Rajan R. RNA-Independent DNA Cleavage Activities of Cas9 and Cas12a. Cell Rep. 2017;21:3728–39.

47. Wimhurst JM, Manchester KL. Comparison of ability of Mg and Mn to activate the key enzymes of glycolysis. FEBS Lett. 1972;27:321–6.

48. Coudray A, Battenhouse AM, Bucher P, Iyer VR. Detection and benchmarking of somatic mutations in cancer genomes using RNA-seq data. PeerJ. 2018;6:e5362.

49. LaFave MC, Varshney GK, Vemulapalli M, Mullikin JC, Burgess SM. A defined zebrafish line for high-throughput genetics and genomics: NHGRI-1. Genetics. 2014;198:167–70.

50. Lindsay H, Burger A, Biyong B, Felker A, Hess C, Zaugg J, et al. CrispRVariants charts the mutation spectrum of genome engineering experiments. Nat Biotechnol. 2016;34:701–2.

51. Sentmanat MF, Peters ST, Florian CP, Connelly JP, Pruett-Miller SM. A Survey of Validation Strategies for CRISPR-Cas9 Editing. Sci Rep. 2018;8:888.

52. Suurväli J, Whiteley AR, Zheng Y, Gharbi K, Leptin M, Wiehe T. The Laboratory Domestication of Zebrafish: From Diverse Populations to Inbred Substrains. Mol Biol Evol. 2020;37:1056–69.

53. Coe TS, Hamilton PB, Griffiths AM, Hodgson DJ, Wahab MA, Tyler CR. Genetic variation in strains of zebrafish (Danio rerio) and the implications for ecotoxicology studies. Ecotoxicology. 2009;18:144–50.

1   54. Westerfield M. The Zebrafish Book: A Guide for the Laboratory Use of Zebrafish (Danio
2   Rerio). 2007.

3   55. Quinlan AR. BEDTools: The Swiss-Army Tool for Genome Feature Analysis. Curr Protoc
4   Bioinformatics. 2014;47:11.12.1–34.

5   56. Van der Auwera GA, Carneiro MO, Hartl C, Poplin R, Del Angel G, Levy-Moonshine A, et
6   al. From FastQ data to high confidence variant calls: the Genome Analysis Toolkit best practices
7   pipeline. Curr Protoc Bioinformatics. 2013;43:11.10.1–11.10.33.

8   57. Jao L-E, Appel B, Wente SR. A zebrafish model of lethal congenital contracture syndrome 1
9   reveals Gle1 function in spinal neural precursor survival and motor axon arborization.
10 Development. 2012;139:1316–26.

11 58. Schindelin J, Arganda-Carreras I, Frise E, Kaynig V, Longair M, Pietzsch T, et al. Fiji: an
12 open-source platform for biological-image analysis. Nat Methods. 2012;9:676–82.

13 59. Lazzarotto CR, Nguyen NT, Tang X, Malagon-Lopez J, Guo JA, Aryee MJ, et al. Defining
14 CRISPR-Cas9 genome-wide nuclease activities with CIRCLE-seq. Nat Protoc. 2018;13:2615–
15 42.

16 60. Li H, Durbin R. Fast and accurate short read alignment with Burrows-Wheeler transform.
17 Bioinformatics. 2009;25:1754–60.

18 61. Wu X, Kriz AJ, Sharp PA. Target specificity of the CRISPR-Cas9 system. Quantitative
19 Biology. 2014;2:59–70. doi:10.1007/s40484-014-0030-x.

20 62. Dobin A, Gingeras TR. Mapping RNA-seq Reads with STAR. Curr Protoc Bioinformatics.
21 2015;51:11.14.1–11.14.19.

22 63. McLaren W, Gil L, Hunt SE, Riat HS, Ritchie GRS, Thormann A, et al. The Ensembl
23 Variant Effect Predictor. Genome Biol. 2016;17:122.

24 64. Andrews S, Others. FastQC: a quality control tool for high throughput sequence data. 2010.

25 65. Bolger AM, Lohse M, Usadel B. Trimmomatic: a flexible trimmer for Illumina sequence
26 data. Bioinformatics. 2014;30:2114–20.

27 66. Patro R, Duggal G, Love MI, Irizarry RA, Kingsford C. Salmon provides fast and bias-aware
28 quantification of transcript expression. Nat Methods. 2017;14:417–9.

29 67. Love MI, Huber W, Anders S. Moderated estimation of fold change and dispersion for RNA-
30 seq data with DESeq2. Genome Biol. 2014;15:550.

31 68. Yu G, Wang L-G, Han Y, He Q-Y. clusterProfiler: an R package for comparing biological
32 themes among gene clusters. OMICS. 2012;16:284–7.

33 69. Zhou G, Soufan O, Ewald J, Hancock REW, Basu N, Xia J. NetworkAnalyst 3.0: a visual

1   analytics platform for comprehensive gene expression profiling and meta-analysis. Nucleic
2   Acids Res. 2019;47:W234–41.

3   70. Xia J, Gill EE, Hancock REW. NetworkAnalyst for statistical, visual and network-based
4   meta-analysis of gene expression data. Nature Protocols. 2015;10:823–44.
5   doi:10.1038/nprot.2015.052.

6   71. Team RC. R: A language and environment for statistical com-puting. 2017.

7   72. Larsson J. eulerr: area-proportional Euler and Venn diagrams with ellipses. R package
8   version. 2018;4.

9   73. pheatmap: Pretty Heatmaps. https://CRAN.R-project.org/package=pheatmap. Accessed 8 Oct
10 2021.

11 74. du Sert NP, Hurst V, Ahluwalia A, Alam S, Avey MT, Baker M, et al. The ARRIVE
12 guidelines 2.0: Updated guidelines for reporting animal research. PLoS Biol. 2020;18:e3000410.

13

14 **FIGURE LEGENDS**

15 **Figure 1. Workflow for the evaluation of CRISPR cleavages in NHGRI-1 zebrafish**

16 **embryos.** **(A)** The cartoon depicts our experiment, which included 50 gRNAs individually

17 microinjected into one-cell stage embryos, DNA extracted from 20 pooled G_0 larvae, and

18 genomic regions targeted by the gRNA amplified. Lightning symbols represent a cleavage event.

19 (B) An *in vivo* score was obtained from the Sanger sequencing traces using the ICE and TIDE

20 tools, with an example output from ICE pictured. **(C)** Scores for the two tools were plotted with

21 values below the median in orange and above the median in purple. **(D)** Scores from ICE and

22 TIDE tools were compared to *in vivo* scores from Illumina sequencing of the same regions. (E)

23 From the PAGE, an empirical intensity ratio was obtained and compared to the *in vivo* scores

24 from Illumina and Sanger sequencing (ICE). Spearman correlations results are shown in the

25 scatter plots with the line of best fit included.

26

27 **Figure 2. Correlation of on-target efficiencies calculated using different methods. (A)**

1   Heatmap of the efficiency scores obtained from the design tool (CRISPRScan), *in silico*

2   prediction tools, and cutting cleavages obtained *in vivo* using Illumina sequencing and a

3   deconvolution tool (ICE) from Sanger sequencing [34] for 50 gRNAs. Each box represents a

4   gRNA and the efficiency scores range from 0 (blue) to 100 (red). **(B)** Spearman correlations

5   between all efficiency scores from in silico predictions, an *in vitro* protocol [28], and *in vivo*

6   cutting assays. Each box includes the correlation result with the p-value in parenthesis. The color

7   of the boxes represent the correlation values, ranging between -1 (blue) and 1 (red). CHOPCHOP

8   scores were obtained using two different scoring methods, CHOPCHOP (D) (based on [39]) and

9   CHOPCHOP (X) (based on [40]).

10

11   **Figure 3. Assessment of off-target cleavage events using different prediction methods. (A)**

12   The number of predicted CRISPRScan off-target sites correlated with the number of identified

13   CIRCLE-seq sites (Spearman correlation). Log normalization was used to reduce the range in the

14   number of sites. **(B)** *In vivo* editing scores from the ICE tool for the top predicted off-target sites

15   using CRISPRScan and CIRCLE-seq were not different. Scores were compared using a Mann-

16   Whitney U test. **(C)** Editing efficiencies at predicted off-target sites using *in vivo* scores from

17   Sanger sequencing and mosaicism % from Illumina sequencing were correlated (Spearman

18   correlation). **(D)** Editing scores obtained *in vivo* at off-target sites were not correlated with the

19   on-target efficiency of the gRNA. All scatter plots include the Spearman correlations results with

20   the line of best fit.

21

22   **Figure 4. Evaluation of spurious genomic mutations in CRISPR-injection controls. (A)** The

23   abundance of protein-coding genes carrying frameshift variants for each Cas9-injected treatment

1   are depicted in a Venn diagram, with mutated genes identified in both treatments listed. **(B)**

2   Genomic DNA from zebrafish larvae injected with Cas9 enzyme, Cas9 mRNA, catalytically

3   dead Cas9 (dCas9), a scrambled gRNA, uninjected batch siblings, and a fin clip from their

4   parents was used to perform targeted Illumina sequencing of 21 genes to quantify indel

5   mosaicism with average ± standard deviation values listed in the table (see Supplementary Table

6   1 and Supplementary Table 7 for the description of the genes).

7

8   **Figure 5. Evaluation of expression variability in CRISPR-injection controls. (A)** Principal

9   components analysis using the transcript abundances in larvae injected with Cas9 enzyme (Enz1,

10 Enz2, Enz3), Cas9 mRNA (RNA1, RNA2, RNA3), uninjected siblings (Uni1, Uni2), and

11 uninjected siblings from a different batch (Uni3, Uni4, Uni5). **(B)** Volcano plots show the

12 differentially-expressed genes in Cas9-enzyme and Cas9-mRNA injected larvae with the number

13 (and %) of upregulated (fold change > 1) and downregulated (fold change < -1) genes. The top

14 five representative up- and downregulated genes are highlighted, with the full list of genes

15 available as Supplementary Table 6. **(C)** Differentially-expressed genes across samples injected

16 with Cas9 enzyme or Cas9 mRNA relative to uninjected batch-siblings show significant

17 correlations. Plots include the numbers and percentages (in parentheses) of genes downregulated

18 (blue) and upregulated (red) in both Cas9 treatments from the total amount of genes assayed (n=

19 30,258).